Three-Dimensional Limit-Equilibrium Stability Analyses of Slopes and Effect of Inclusion of Soil Nails

P. K. Basudhar[1]; Anubhav[2]; and M. R. Lakshminarayana[3]

Abstract: This study undertook stability analysis of nailed soil slopes using the limit-equilibrium method (LEM) and considering a three-dimensional (3D) rigid-body rotational failure mechanism with the assumed slip surface being a part of a sphere. The moment equilibrium of the 3D wedge formed by the slope surface and the slip surface along with the nails embedded in it were analyzed as a whole. A specific-purpose computer code was written for factor-of-safety (FS) computation; the developed computer code is capable of analyzing an unreinforced slope and a nailed slope. The critical slip surface and the corresponding minimum FS value of the unreinforced slope were initially determined, taking into account all possibilities of failure (base failure, slope failure, and toe failure). For the critical slip surface so obtained, nails were then introduced at desired positions, and the FS value for the nailed slope was then estimated with the developed procedure. The developed method and computer code were verified by comparing the FS values of some benchmark problems [two-dimensional (2D) and 3D] obtained by the proposed method with those reported in the literature. The critical slip surfaces obtained from the proposed method were also compared with some of the benchmark problems. A parametric study was conducted to determine the effects of the inclination and spacing of the nails on the FS values. **DOI: 10.1061/(ASCE)GM.1943-5622.0000932.** *© 2017 American Society of Civil Engineers.*

Author keywords: Limit-equilibrium method; Reinforced slope; Soil nailing; Three-dimensional (3D) analysis.

Introduction

For infrastructural developments in congested urban areas, it is often necessary to excavate soils either vertically or with steep slopes that may not have an adequate factor of safety (FS). Soil nailing is a very common technique that is generally adopted for such slopes so that the FS is increased to the desired level. In recent years, soil nailing has gained momentum all over the world as a preferred, popular, and cost-effective method for construction of such steep-cut slopes and also in the in situ stabilization of natural slopes. The construction process of soil nailing and installation of the nails is extremely flexible and allows for adjustment of nail directions to maximize the reinforcing action. Soil nailing can be effectively implemented in natural cohesive materials, such as silty clays, low-plasticity clays, and naturally cemented sand/gravel deposits. It is not recommended for sands and gravel without cohesion, organic clays, or expansive and swelling soils (Lazarte et al. 2003).

Several methods are available for analysis and design of nailed slopes based on limit-equilibrium, limit-analysis, finite-element, and finite-difference methods. The limit-equilibrium method (LEM) gained more popularity among practicing engineers because of its reasonable accuracy and simplicity. Assuming plane-strain conditions, two-dimensional (2D) LEM is generally used to analyze such slopes for stability computations (Juran et al. 1990; Maleki and Mohammad 2012; Patra and Basudhar 2005; Rotte et al. 2011; Sabhahit et al. 1995; Wright and Duncan 1991; Yuan et al. 2003). Very often, the 2D analyses do not correctly represent the failure mode, are conservative, and underestimate the FS (Hovland 1977; Chen and Chameau 1983), which may result in a costly design. Three-dimensional (3D) studies have also been carried out for nailed slopes using finite-element and finite-difference methods (Wei and Cheng 2010; Zhang et al. 1999; Halabian et al. 2012). Some 3D LEMs were developed in the past for unreinforced slopes (Anagnosti 1969; Baligh and Azzouz 1975; Hovland 1977; Chen and Chameau 1983; Leshchinsky and Huang 1992; Lam and Fredlund 1993; Ahmed et al. 2012). Analyses of unreinforced slopes show that 3D FS values are generally greater than the corresponding 2D FS values (Hovland 1977; Wei et al. 2009; Chen and Chameau 1983; Baligh and Azzouz 1975 etc.). In some cases, however, 3D FS values were reported to be less than the corresponding 2D values (Hovland 1977; Chen and Chameau 1983). Therefore, 3D analysis is also desirable in these cases for safety considerations.

An overview of the literature shows that little attention has been given to simpler 3D LEM-based stability analyses of nailed slopes. Thus, this study developed a simple analytical procedure based on limit equilibrium for the 3D analysis of unreinforced slopes that can be further extended to compute the FS values of nailed soil slopes. This method of analysis can be adopted for the preliminary design of such slopes, and the chosen design may be checked with finite-element analysis to determine if the deformations are within permissible limits.

Analysis

A soil slope of height h_s with inclination α with the horizontal is shown in Fig. 1. To increase the stability of the slope, nails were

[1]Visiting Faculty, Civil Engineering Dept., Indian Institute of Technology (BHU), Varanasi 221005, India; formerly, Professor, Dept. of Civil Engineering, Indian Institute of Technology Kanpur, Kanpur 208016, India (corresponding author). E-mail: pkbd@iitk.ac.in

[2]Deputy General Manager, Solapur Super Thermal Power Project, NTPC Ltd., Solapur 413215, India. E-mail: anubhav@ntpc.co.in

[3]Vice President, Operations and Delivery, Niranta Solutions and Services Pvt. Ltd. (NSSPL), Bangalore 560102, India. E-mail: lakshminarayana.mr@niranta.in

Note. This manuscript was submitted on February 18, 2016; approved on February 7, 2017; published online on June 7, 2017. Discussion period open until November 7, 2017; separate discussions must be submitted for individual papers. This paper is part of the ***International Journal of Geomechanics***, © ASCE, ISSN 1532-3641.

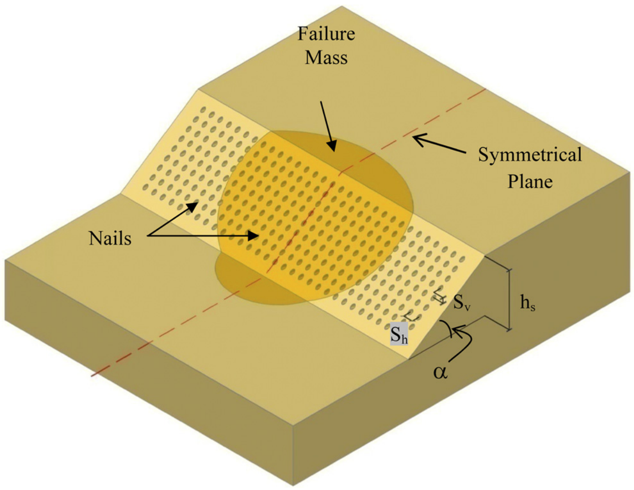

Fig. 1. 3D failure mass with nails

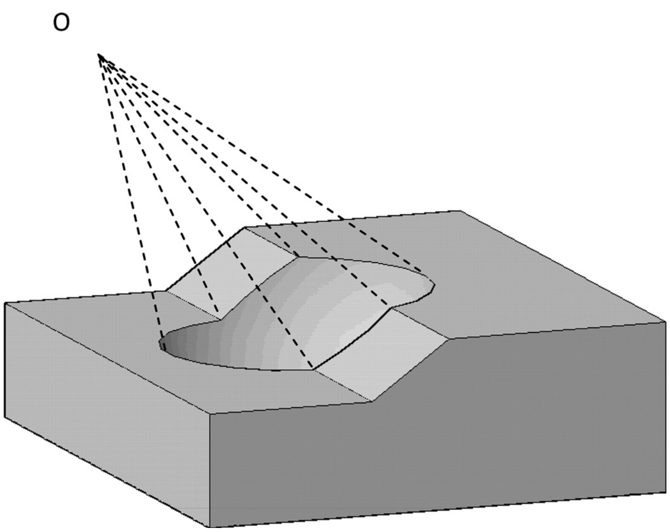

Fig. 2. 3D view of failure surface

driven in the slope at an angle, η, with horizontal and vertical spacings of S_h and S_v, respectively.

For determining the critical slip surface and the corresponding value of the minimum FS, the problem was cast as a mathematical programming problem. The trial slip surfaces were assumed to be part of a sphere. The analysis was based on the following assumptions:

1. The rotational failure of the wedge is bounded by the slope surface, and the slip surface is spherical in shape (Figs. 2 and 3).
2. The soil is homogeneous and isotropic.
3. Failure could occur by any of the following modes: base failure, slope failure, and toe failure.

The forces acting on the free body of the failure wedge (sectional view of the symmetrical plane) are shown in Fig. 3. The analysis was carried out considering the equilibrium of the free body as a whole. The method of analysis presented in this paper follows the basic procedure developed earlier by Lakshminarayana (1997).

The cohesive force is assumed to act at the point where the vertical line drawn through the center of gravity of the sliding block intersects the slip surface. Considering the moment of all forces about the rotational axis, the FS of the nailed slope can be expressed as

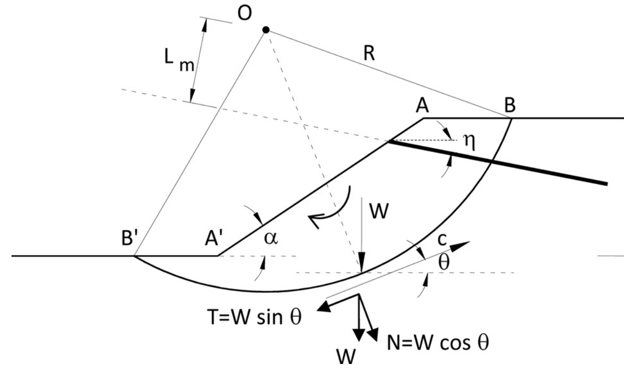

Fig. 3. Free-body diagram of failure block

$$\mathrm{FS} = \frac{R\left[c'A_s + \tan\,\varphi'(W\cos\theta)\right] + \sum(N_f)(L_m)}{RW\sin\theta} \tag{1}$$

where R = radius of spherical failure surface; A_s = surface area of failure mass; W = weight of sliding mass; θ = angle made by the tangent drawn at the intersection of the vertical line drawn through the center of gravity of the sliding mass and slip surface, with horizontal; N_f = tensile force contribution from each nail; L_m = perpendicular distance from the direction of the nail force to the axis of rotation of the sliding mass; c' = effective cohesion of soil; and φ' = angle of shearing resistance of soil.

The analysis was carried out in two steps. First, the mathematical model was developed for determining the critical FS and the corresponding failure surface for an unreinforced slope. Then nails were introduced in the stability analysis for calculation of the enhanced FS of nailed slopes.

Computation of Geometrical Parameters of Failure Mass

A sectional view of the symmetrical plane of the 3D slope is shown in Fig. 4. If X, Y, and Z represent any arbitrary point on the spherical slip surface (shown as a circle in the cross section in Fig. 4) with X_c, Y_c, and Z_c as its center, the equation can be expressed as follows:

$$(X - X_c)^2 + (Y - Y_c)^2 + (Z - Z_c)^2 = R^2 \tag{2}$$

For simplicity, the symmetrical plane of an arbitrary spherical failure surface is assumed to be lying on the xy-plane. The center of the failure surface is $p(X_c, Y_c, 0)$. To make the formulation simpler, a local coordinate system has been considered in which the origin is at the center of rotation of the sliding mass. The details of the transformation of the coordinate system are shown in Fig. 4. The transformed equation of the sphere in the local coordinate system with radius R will be

$$x^2 + y^2 + z^2 = R^2 \tag{3}$$

With the failure mass being symmetrical about the z-axis, the z-coordinate of the sphere and planes will not appear in the equations for calculation of the FS.

Let the coordinates of the crest and toe of the slope in the global coordinate system be $A(X_1, Y_1)$ and $A'(X_2, Y_2)$, respectively. For transformation into the local coordinate system, the relationship between the coordinates of these points can be expressed as

Int. J. Geomech., 2017, 17(9): 04017067

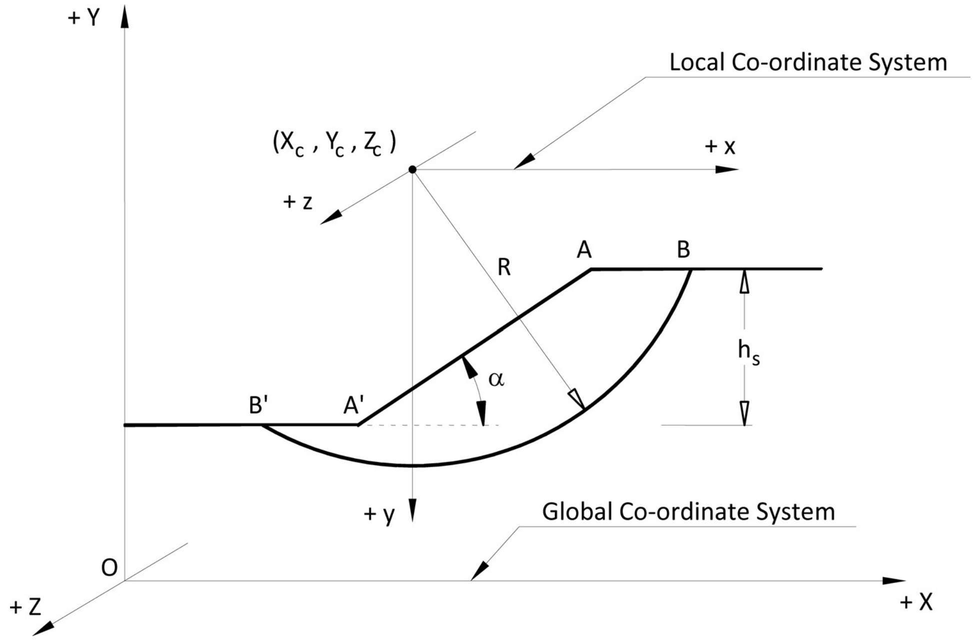

Fig. 4. Global and local coordinate system

$$x_1 = X_1 - X_c,\ x_2 = X_2 - X_c \tag{4}$$

$$y_1 = Y_1 - Y_c \qquad y_2 = Y_2 - Y_c \tag{5}$$

where $A(x_1, y_1)$ and $A'(x_2, y_2)$ are in the local coordinate system.

To determine the FS for any spherical slip surface, the required parameters are as follows:

- Total weight of soil bounded by crest plane, inclined plane, bottom plane, and spherical surface (W) from the volume computation
- Center of gravity (CG) of the soil mass (W) with respect to the y-axis
- Surface area of the failure block

The geometrical parameters (i.e., volume, surface area, and CG of the failure block) required for obtaining the FS can be computed by dividing the symmetrical section (Fig. 5) into three parts: CBC', ABC, and $A'B'C'$. If the volumes of CBC', ABC, and $A'B'C'$ are represented by V_1, V_2, and V_3, respectively, then the total volume (V) of the failure block $ABC'B'A'$ is given by

$$V = V_1 - V_2 + V_3 \tag{6}$$

Similarly, the net surface area of the failure block can be expressed as

$$A_s = A_{s1} - A_{s2} + A_{s3} \tag{7}$$

If the distance of the CGs of the parts CBC', ABC, and $A'B'C'$ from the y-axis are CG_1, CG_2, and CG_3, respectively, then the CG of the failure block can be expressed as

$$\mathrm{CG} = \frac{(\mathrm{CG}_1)(V_1) - (\mathrm{CG}_2)(V_2) + (\mathrm{CG}_3)(V_3)}{V_1 - V_2 + V} \tag{8}$$

Part CBC′

Fig. 6 shows CBC', which is formed as inclined plane cuts the sphere at a distance d from the center of rotation. Consider an axis L with origin at the center of the sphere and passing perpendicular to the plane CC'. The volume of an element with thickness dl at a distance l from the origin is given by

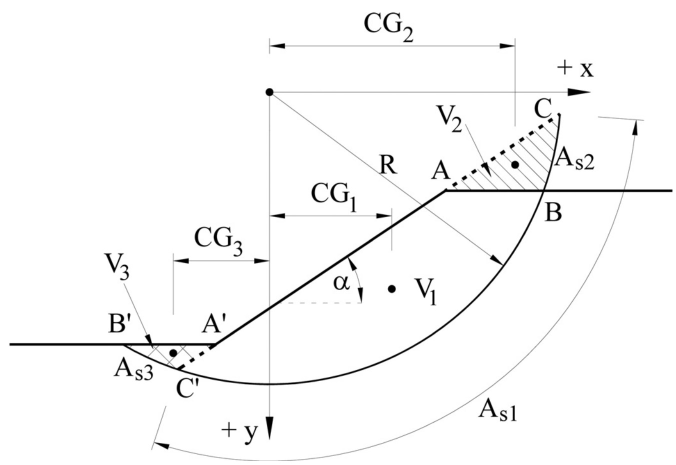

Fig. 5. Scheme for computation of the surface area: discretization of failure block

$$dv = \pi\left(\sqrt{R^2 - l^2}\right)dl \tag{9}$$

The volume of CBC' can be obtained by integrating Eq. (9) as

$$V_1 = \int_d^R \pi\left(\sqrt{R^2 - l^2}\right)dl \tag{10}$$

On simplification, Eq. (10) becomes

$$V_1 = \frac{\pi}{3}(2R^3 - 3R^2 d + d^3) \tag{11}$$

Similarly, the moment of inertia of the elemental volume dv about O is given by

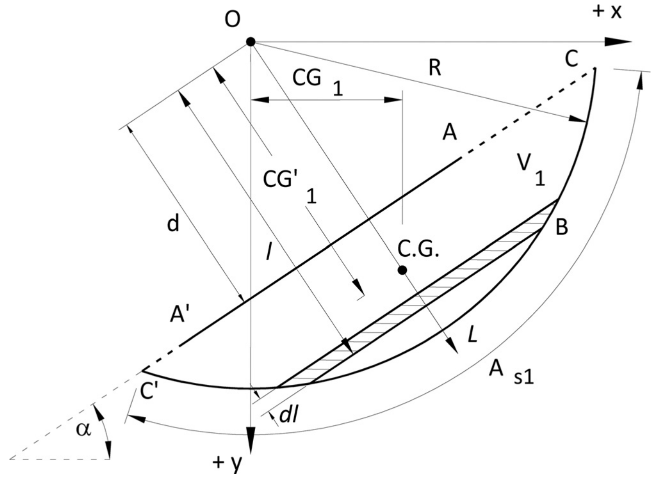

Fig. 6. Part CBC′

$$dM = l\pi\left(\sqrt{R^2 - l^2}\right)^2 dl \tag{12}$$

and the moment of inertia of CBC' is given by integrating Eq. (12) as

$$M_1 = \int_d^R l\pi\left(\sqrt{R^2 - l^2}\right)^2 dl = \frac{\pi}{4}(R^4 - 2R^2d^2 + d^4) \tag{13}$$

The distance of the CG of CBC' from center O along axis L can be computed as

$$\mathrm{CG}_1' = \frac{M_1}{V_1} = \frac{\int_d^R l\pi\left(\sqrt{R^2 - l^2}\right)^2 dl}{\int_d^R \pi\left(\sqrt{R^2 - l^2}\right) dl} = \frac{3\cdot(R^4 - 2R^2d^2 + d^4)}{4\cdot(2R^3 - 3R^2d + d^3)} \tag{14}$$

Now, the distance of the CG of CBC' from the y-axis can be obtained as

$$\mathrm{CG}_1 = (\mathrm{CG}_1')\sin\alpha \tag{15}$$

The surface area of CBC' can be evaluated by

$$A_{s1} = 2\pi R(R - d) \tag{16}$$

Parts ABC *and* A′B′C′

For the derivation of expressions for calculating geometric parameters, ABC and $A'B'C'$ can be considered as the volume between the boundary of the sphere and two planes that intersect at an angle α (Fig. 7).

AC and AB are two planes that intersect at an angle α at the point $A(x_1, y_1)$ inside a sphere of radius R. The volume bounded between the inclined plane AB, the horizontal plane AC, and the sphere boundary can be given by

$$V_2 = \int_{y_1}^{y_t}\int_{\left(\frac{y-y_1}{\tan\alpha}-x_1\right)}^{\sqrt{R^2-y^2}}\int_{-\sqrt{R^2-x^2-y^2}}^{\sqrt{R^2-x^2-y^2}} dz\,dx\,dy \tag{17}$$

where y_t is the y-coordinate of the point C (Fig. 7).

Eq. (17) can be simplified as

$$V_2 = 2\int_{y_1}^{y_t}\int_{\left(\frac{y-y_1}{\tan\alpha}-x_1\right)}^{\sqrt{R^2-y^2}}\left(\sqrt{R^2 - x^2 - y^2}\right)dx\,dy \tag{18}$$

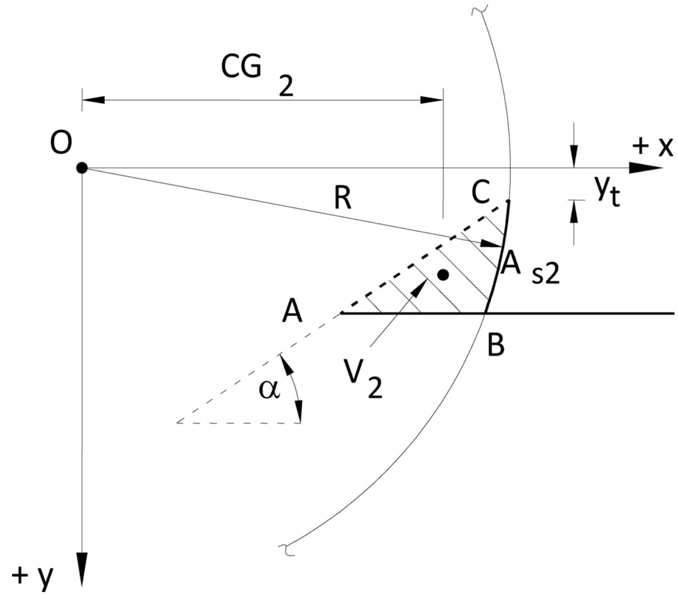

Fig. 7. Part ABC of failure block

For integration of Eq. (18), the inner limits of integration are changed to 0 and 1, as follows:

$$\int_a^b\int_{g_1(y)}^{g_2(y)} f(x,y)\,dx\,dy = \int_a^b\int_0^1 f[(1-v)\cdot g_1(u) + v\cdot g_2(u), u][g_2(u) - g_1(u)]\,du\,dv \tag{19}$$

where, $y = u$; and $x = (1-v)\cdot g_1(u) + v\cdot g_2(u)$.

Using Eq. (18), the volume V_2 can be expressed as

$$V_2 = 2\int_{y_1}^{y_t}\int_0^1\left\{\sqrt{R^2 - \left[(1-\nu)\cdot\left(\frac{y-y_1}{\tan\alpha} - x_1\right) + \nu\cdot\sqrt{R^2-y^2}\right]^2 - u^2}\right\}\cdot\left[\sqrt{R^2-y^2} - \left(\frac{y-y_1}{\tan\alpha} - x_1\right)\right]du\,dv \tag{20}$$

Eq. (20) is integrated numerically using Simpson's rule. Similarly, the moment of inertia of the part ABC can be expressed as

$$M_2 = 2\int_{y_1}^{y_t}\int_{\left(\frac{y-y_1}{\tan\alpha}-x_1\right)}^{\sqrt{R^2-y^2}} x\cdot\left(\sqrt{R^2 - x^2 - y^2}\right)dx\,dy \tag{21}$$

The inner limits of integration of Eq. (21) are also converted to 0 and 1, as in the case of Eq. (18), and then numerically integrated using Simpson's rule.

The distance of the CG of the volume of ABC from the y-axis can be evaluated as

$$\mathrm{CG}_2 = \frac{M_2}{V_2} \tag{22}$$

In Eqs. (20) and (21), y_t is the y-coordinate of the point C. The equation of the plane AC that is passing through the point $A(x_1, y_1)$ and making an angle α (slope $i = \tan\ \alpha$) with the horizontal is given by

$$y - y_1 = i(x - x_1) \tag{23}$$

Substituting Eq. (23) in the equation of sphere gives

$$x^2 + [y_1 + i(x - x_1)]^2 = R^2 \tag{24}$$

Solving Eq. (24), x can be obtained as

$$x = \frac{-2i(y_1 - i \cdot x_1) \pm \sqrt{[2i(y_1 - i \cdot x_1)]^2 - 4 \cdot [1 + i^2] \cdot \left[(y_1 - i \cdot x_1)^2 - R^2\right]}}{2(1 + i^2)} \tag{25}$$

Substituting a positive value of x in Eq. (23), the y-coordinate of the point $C\,(y_t)$ can be obtained.

The adopted procedure for evaluating the surface area of ABC is described herein. If the surface equation $F(x, y, z) = c$ lying above the projection R on a ground plane directly beneath it, then the surface area is given by

$$S' = \iint \frac{|\nabla F|}{|\nabla F \cdot n|} da \tag{26}$$

where S' = surface area; n = unit vector normal to the ground plane; da = elemental area; and ∇F = gradient of function $F(x, y, z) = c$, as follows:

$$\nabla F = \left(\hat{i}\frac{\partial}{\partial x} + \hat{j}\frac{\partial}{\partial y} + \hat{k}\frac{\partial}{\partial z}\right) F(x, y, z) \tag{27}$$

in the present case, that is

$$F(x, y, z) = x^2 + y^2 + z^2 \tag{28}$$

Eqs. (27) and (28) give

$$\nabla F = 2x\hat{i} + 2y\hat{j} + 2x\hat{k} \tag{29}$$

$$|\nabla F| = 2\sqrt{x^2 + y^2 + z^2} = 2R \tag{30}$$

$$|\nabla F \cdot n| = 2z = 2\sqrt{R^2 - y^2 - x^2} \tag{31}$$

Therefore, the surface area is given by

$$A_{s2} = \int_{y_1}^{y_t} \int_{x_1}^{\sqrt{R^2 - y^2}} \left(\frac{R}{\sqrt{R^2 - x^2 - y^2}}\right) dx dy \tag{32}$$

By substituting $x = (\sqrt{R^2 - y^2}) \sin\theta$ and $dx = (\sqrt{R^2 - y^2}) \cos\theta\, d\theta$, Eq. (32) can be simplified as

$$A_{s2} = R \cdot \int_{y_1}^{y_t} \left[\frac{\pi}{2} - \arcsin\left(\frac{x_1}{\sqrt{R^2 - y^2}}\right)\right] dy \tag{33}$$

which can be further simplified to

$$A_{s2} = \frac{\pi}{2} R \cdot (y_t - y_1) - R \int_{y_1}^{y_t} \left[\arcsin\left(\frac{x_1}{\sqrt{R^2 - y^2}}\right)\right] dy \tag{34}$$

Eq. (34) for calculating surface area is integrated numerically using Simpson's rule. It can be seen that $A'B'C'$ is similar to ABC, and therefore the geometric parameters can be calculated with the methods that are applied for part ABC.

From this mathematical formulation, various geometrical parameters for assumed failure mass (base failure, toe failure, or face failure) required to compute the FS value can be obtained.

Effective Length and Lever Arm of Nails

The total length of the nail to be provided is the length of the nail within failure surface l_a and the length of the nail anchored beyond the failure surface l_e, as follows:

$$L = l_a + l_e \tag{35}$$

To determine the length of the nail beyond the slip surface, the following procedure is used. Let the nail be placed at a point $p(nx, ny, nz)$ on the inclined surface of the slope and at an angle η with the horizontal. Let $q(c, d)$ be the point at which the nail intersects the critical slip surface. For these calculations, the local coordinate system has been considered with (0, 0, 0) as the center of the slip surface (local coordinate system as per Fig. 4). The radius of the circle at distance nz from the origin, which falls on the external surface of a sphere, can be written as $R_n = \sqrt{R^2 - (nz)^2}$, and the equation of the circle at the location of the nail is given by

$$x^2 + y^2 = R_n^2 \tag{36}$$

The equation of the line along the nail can be written as

$$y - ny = (x - nx)\tan\eta \tag{37}$$

Let $\tan\ \eta = n_i$; then Eq. (38) becomes

$$y - ny = (x - nx)n_i \tag{38}$$

Solving Eqs. (36) and (38) for x gives

$$x = \frac{-2n_i(ny - n_i \cdot nx) \pm \sqrt{\left[2n_i(ny - n_i \cdot nx)\right]^2 - 4\left(1 + n_i^2\right)\left[(ny - n_i \cdot nx)^2 - R_n^2\right]}}{2\left(1 + n_i^2\right)} \tag{39}$$

Int. J. Geomech., 2017, 17(9): 04017067

By substituting a positive value of x in Eq. (38), the value of y can be obtained. The value of (x, y) will be the coordinate at which the nail intersects the critical slip surface [i.e., $q(c, d)$]. Now the length of the nail within the slip surface is given by

$$l_a = \sqrt{(nx - c)^2 + (ny - d)^2} \tag{40}$$

The effective length of the nail can be obtained from Eq. (35). Now the perpendicular distance of the nail from the center of rotation (0,0) can be obtained from the following equation:

$$l_m = \frac{(-n_i \cdot nx + ny)}{\sqrt{n_i^2 + (-1)^2}} \tag{41}$$

The computer program for the computation of the coordinates, effective length of nails, and so forth was verified by plotting the geometry of the slope, slip circle, and nails in *AutoCAD*.

Tensile Force from Nails

Only the tensile resistance of the reinforcement is included, and the effect of shear and bending is neglected. The tensile force T_n in a nail is given by

$$T_n = \pi \cdot d_e \cdot l_e \cdot \tau_{\text{bond}} \tag{42}$$

where d_e = nail/hole diameter; l_e = length of the nail anchored beyond the failure surface; and τ_{bond} = bond stress between nail/grout and soil.

The tensile force must be less than the yield strength of the nail T_y. This condition has been kept as a constraint in the computer program.

$$T_n \le T_y \tag{43}$$

It may be noted that as per Federal Highway Administration (FHWA) guidelines (Lazarte et al. 2003), the tensile force of the nail increases at a constant slope equal to the pullout capacity per unit length, reaches a maximum value $T_{\max}$, and then decreases to the value T_0 at the nail head [Fig. 8(a)]. However, to simplify the computer code, the tensile force distribution was slightly modified by ignoring the force at the nail head [Fig. 8(b)].

In the analysis of a nailed soil structure, the most critical parameter is the limiting bond stress (τ_{bond}). The maximum bond stress available between a nail and soil is a function of the surface of the nail, the nature of the soil, and the in situ stress in the soil. Cohesive soils tend to offer a lower bond resistance than granular soils. Nails that are grouted rather than those driven into ground typically provide a better bond with soil. Pullout tests should be conducted to establish the value of bond stress for design. However, in the absence of pullout test data, the designer may make an estimate of the pullout resistance, which will be verified at the time of construction. The bond stress varies with the depth of overburden, and in the absence of any pullout test data, the bond stress for a nail can be calculated by the following equation:

$$\tau_{\text{bond}} = c_i + \gamma \cdot d_j \cdot \tan\ \varphi_i \tag{44}$$

where c_i = adhesion intercept at interface between nail and soil; ϕ_i = interface friction between nail and soil; γ = unit weight of soil; and d_j = average depth of soil lying above effective length of jth nail (Fig. 9).

Evaluation of Minimum FS and Critical Slip Surface

Using the developed procedure, a computer code was developed in *MATLAB* to determine the FS for the unreinforced slope, as follows:

$$\text{FS} = \frac{R\left[c' A_s + \tan\ \varphi' (W \cos\ \theta)\right]}{RW \sin\ \theta} \tag{45}$$

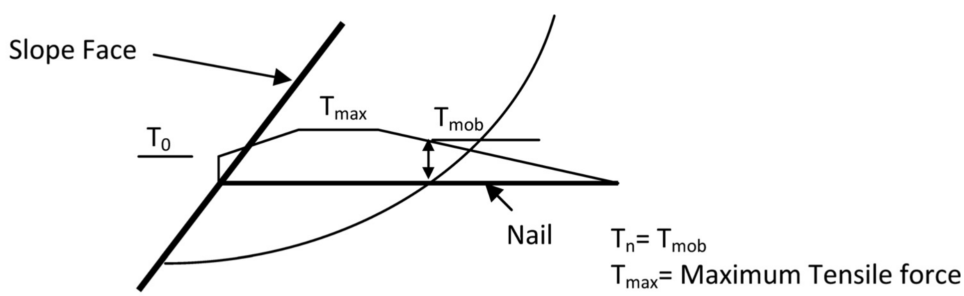

(a)

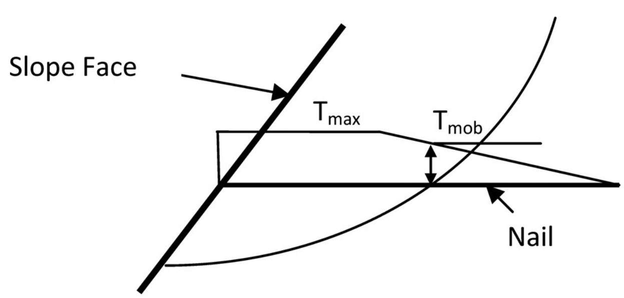

(b)

Fig. 8. Tensile force distribution in nail: (a) FHWA guidelines; (b) considered in present analysis

Int. J. Geomech., 2017, 17(9): 04017067

The critical FS was obtained by minimizing the objective function [Eq. (45)] using the optimization scheme *fminsearch* available in *MATLAB*; *fminsearch* uses the Nelder–Mead simplex algorithm as described by Lagarias et al. (1999). Optimization Toolbox 4 in the *MATLAB* user's guide (MathWorks 2017) may be referred to for details of this function. For computation of the FS for the given soil parameters and slope geometry, the design variables were the coordinate of the center (X_c, Y_c) and the radius of the slip surface (R). Because the trial slip surfaces were considered symmetrical about the xy-plane, the z-coordinate of the center was not required as a design variable. While searching for the critical slip surface, geometric and behavior constraints were imposed so that the slip surface was physically possible and the computations made would be meaningful. Corresponding to this critical failure surface, nails were introduced in the slope, and the FS values for nailed slopes were calculated using Eq. (1).

Validation of the Developed Procedure

The developed computer program was checked for its correctness by hand calculations at different stages. The geometric parameters were checked by plotting the slope, slip circle, and other features and measuring the distances to the scale on *AutoCAD*. The program was also validated by working through selected problems available in the literature and comparing the solutions with those obtained by the developed method. The comparisons were also made with the 2 D solutions obtained through some of the latest software.

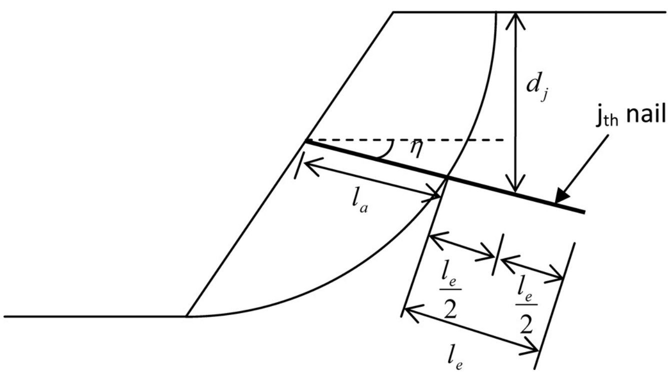

Fig. 9. Active length of nail

To compare the FS values of an unreinforced slope obtained using the proposed method with 2D analysis, a problem previously solved by Chang (1992) was taken up, where a slope of 12 m (40 ft) in height (2 H:1 V) with the soil parameters $c' = 28$ kN·m^2 and $\varphi' = 20°$ and a unit weight of soil of 19.68 kN·m^3 was considered (Case 1). Chang (1992) reported the 2D FS of this slope computed using the then-available various LEM and discrete-element techniques. As a part of the present study, the same slope was analyzed using the 2D LEM analysis program *GEO5* and the program *FLAC/Slope 5*, which is based on a strength-reduction technique (SRT). The obtained FS values were then compared with those reported by Chang (1992) and the proposed 3D method (Table 1). The FS values computed with the presently available software programs were lower than those reported by Chang (1992). Because of this variation in the results, two more problems initially solved by Chen and Chameau (1983) and reported by Hungr (1987) for a 6.1-m-high slope (2.5 H:1 V) were considered for analysis. In the first case, the properties of the homogenous soil were $c' = 14.4$ kN·m^2 and $\varphi' = 25°$ (Case 2), and for the second problem, the soil properties were $c' = 28.7$ kN·m^2 and $\varphi' = 15°$ (Case 3). For both problems, the unit weight of soil was taken as 20 kN·m^2. The results of various analyses for both problems are presented in Tables 2 and 3, respectively.

Tables 2 and 3 show that the FS values computed using the latest software programs were lower than those reported in the literature. Therefore, for comparison purposes, the results of the simplified Bishop's method obtained by *GEO5* are used for all cases presented in this paper. From the comparison of the FS values computed with the 3D analysis method as proposed, it can be seen that the 3D analysis gave 4.79 and 4.66% higher FS values for Case 1 (Table 1) and Case 2 (Table 2), respectively, compared with those of the 2D analysis. For Case 3 (Table 3), the 3D FS was 10.36% higher than the 2D FS. It has been reported that 3D analysis generally produces 10 to 20% higher FS values than the corresponding values obtained by 2D analysis. Thus, the differences found were less than those reported in the literature, and the 3D analysis of the unreinforced slope as computed may be considered to be correct.

Table 1. Comparison of FS Values Obtained from Different Methods—Case 1

	FS (2D)			FS (3D)	
		Present analysis			
Method	Literature (Chang 1992)	*GEO5* (LEM)	*FLAC/Slope 5* (SRT)	Lakshminarayana (1997)	Present analysis
Ordinary	1.93	1.84	1.93	2.26	2.03
Simplified Bishop's	2.08	1.94			
Spencer's	2.07	1.94			
Janbu's	2.04	—			
Discrete element	1.92	—			

Table 2. Comparison of FS Values Obtained from Different Methods—Case 2

	FS (2D)			FS (3D)	
		Present analysis			
Method (LEM)	Literature (Hungr 1987)	*GEO5* (LEM)	*FLAC/Slope 5* (SRT)	Lakshminarayana (1997)	Present analysis
Ordinary	—	2.37	2.56	2.81	2.65
Simplified Bishop's	2.76	2.53			
Spencer's	—	2.53			

Int. J. Geomech., 2017, 17(9): 04017067

Further, for Cases 2 and 3, the slip surfaces obtained from different methods were compared with the symmetrical plane of the failure mass obtained by the proposed method (Fig. 10). For Case 2, the slip surface obtained by the proposed method was deeper than that obtained by the simplified Bishop's method but close to the slip surfaces obtained by Chen and Chameau (1983) and by the ordinary method of slices. A major part of the slip surface fell in the failure zone that was predicted by *FLAC/Slope 5* (2D). Similar observations were noted for Case 3 also. In this case, the slip surface obtained by the proposed method was deeper than that obtained by Chen and Chameau (1983) and the simplified Bishop's method (present analysis); however, it was very close to that obtained by the ordinary method of slices (Fig. 10).

For validation of the proposed method, the problem solved by Chen and Chameau (1983) using 2D and 3D methods (both LEM and FEM) was also considered. The stability analysis was performed for a 9-m-high embankment with a slope of 1.5 H: 1 V. The soil was homogeneous, with a unit weight of 19 kN·m^3 and the soil properties $c' = 34.5$ kN·m^2 and $\phi' = 6°$. The results of various analyses for the problem are presented in Table 4.

The 3D FS obtained with the proposed method was 10.3% lower compared with that obtained by Chen and Chameau (1983) using FEM. It was 10.1 and 15.3% lower than the values obtained by

Table 3. Comparison of FS Values Obtained from Different Methods—Case 3

Method	FS (2D)			FS (3D)	
		Present analysis			
	Literature (Hungr 1987)	*GEO5* (LEM)	*FLAC/Slope 5* (SRT)	Lakshminarayana (1997)	Present analysis
Ordinary	—	2.57	2.72	3.20	3.00
Simplified Bishop's	2.87	2.72			
Spencer's	—	2.72			

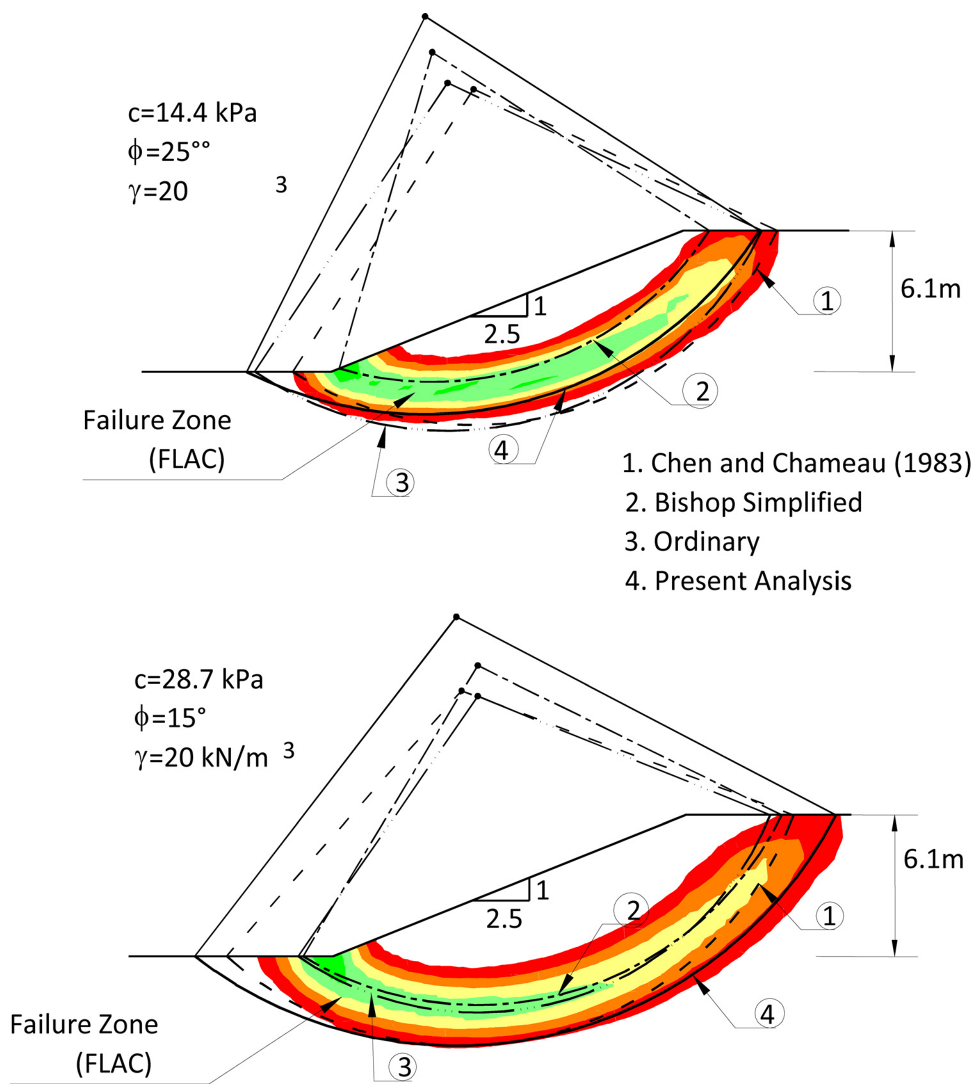

Fig. 10. Comparison for failure surfaces obtained from different methods

Int. J. Geomech., 2017, 17(9): 04017067

Table 4. Comparison of FS Values Obtained from Present Analysis and 3D Analysis Available in the Literature

Method	FS (2D)			FS (3D)		
		Present analysis		Literature		
	Literature (Chen and Chameau 1983)	*GEO5* (LEM)	*FLAC/Slope 5* (SRT)	Chen and Chameau (1983)	Lakshminarayana (1997)	Present analysis (LEM)
LEM	1.59 (Spencer's)	1.58 (Spencer's/simplified Bishop's)	—	1.90	1.90	1.70
FEM/FDM	1.62	—	1.57	2.01	Lakshminarayana (1997)	Lakshminarayana (1997)

Lakshminarayana (1997) and Chen and Chameau (1983), respectively, using LEM. However, the FS value calculated by the proposed 3D method was approximately 5 to 8.5% higher than the values obtained by 2D methods (LEM, FEM, and SRT). In all cases, the FS values obtained from the proposed 3D analysis were found to be higher compared with those obtained by 2D analysis.

Parametric Analysis of Nailed Slopes

A 9-m-high, homogeneous soil slope with an angle of 50° was considered for the analysis of a nailed slope (Fig. 11). The soil parameters as described previously for Case 2 were considered in the analysis. It was assumed that the soil slope would be reinforced by 6-m-long, 25-mm-diameter nails (steel, $f_y = 500$ MPa) and that the nails would be installed horizontally by cement grouting in 150-mm-diameter holes. Chu and Yin (2005, 2006) conducted laboratory pullout tests and interface shear tests on a cement-grouted nail and surrounding soil. Most of the results showed that the cohesion and friction angle for the soil–nail interface were almost the same as the cohesion and friction angle of soil. It has also been reported that the shear stress–displacement behavior of the soil–grout interface showed behavior similar to that of soil alone. Based on the interface shear test between compacted, completely decomposed granite (CDG) soil and cement grout, Hossain and Yin (2014) also reported that a compacted CDG soil–cement grout interface behaves as a rough interface. Therefore, in the present analysis, the interface cohesion and friction angle were considered the same as those for soil. However, in many conditions, the interface shear strength between the nail and soil may be lower than the soil shear strength (Pradhan et al. 2006).

With the proposed 3D analysis method, the FS of the unreinforced slope was found to be 1.051. After incorporating nails with horizontal and vertical spacings of 1 m, the FS was increased to 1.321.

The inclination of the nails affects the FS values of the nailed slopes. Soil nails are generally installed at 10–20° from horizontal. A nail inclination of less than 10° should be avoided to ensure effective grouting, and nails with an inclination that is too steep (more than 40–45°) may be in compression and do not contribute to stability (Lazarte et al. 2003). However, to investigate the effects of the inclination of the nails on the FS for parametric study. the inclination was varied from 0 to 50°. For a 9-m-high 50° slope, the FS increased from 1.55 to 1.76 with an increase in nail inclination from 0 to 25° and then decreased to 1.43 on a further increase of nail inclination to 50°.

To study the effect on nail inclination along with slope angle, the slope angle was also varied from 50 to 30°. Fig. 12 shows the variation of the FS with nail inclination for different slope angles. It was found that optimum nail inclination changed with a change in slope angle. For the slope under consideration, the FS increased

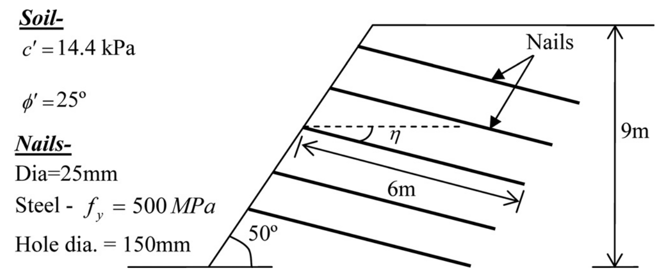

Fig. 11. Section of soil-nailed slopes

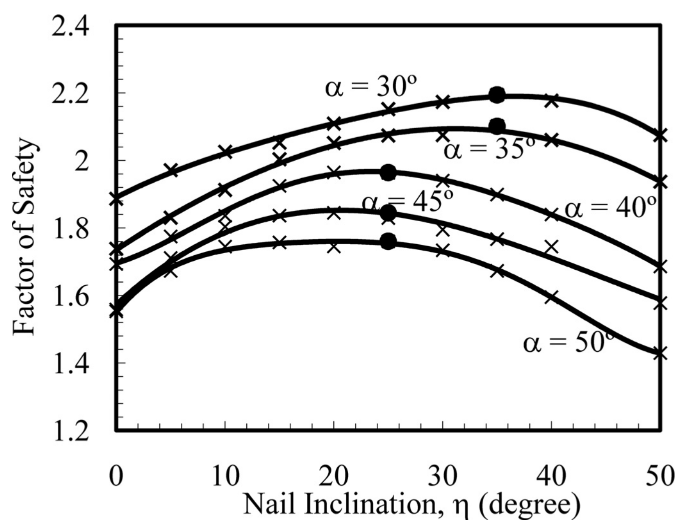

Fig. 12. Influence of nail inclination and slope angle on FS values of soil-nailed slopes

with an increase in nail inclination from 0 to 25° and then decreased with a further increase of nail inclination for 50, 45, and 40° slope. However, for lower slope angles (35 and 30°), the FS increased for nail inclinations from 0 to 35° and then decreased.

To study the effect of slope angle on the increase in the FS values of a reinforced slope with respect to an unreinforced slope, the FS values computed for optimum nail inclination were plotted against slope angles (Fig. 13). It was found that an increase in the FS value of a reinforced slope with respect to an unreinforced slope increased with slope angle.

For a given slope geometry, soil parameters, and nail inclination, the effect of nail spacing on the FS was studied. From the previous problem, a slope with a 40° angle and a nail inclination of 25° (optimum angle) was considered. In general, nails are placed in a grid pattern with equal spacing in both directions, and a minimum of

Int. J. Geomech., 2017, 17(9): 04017067

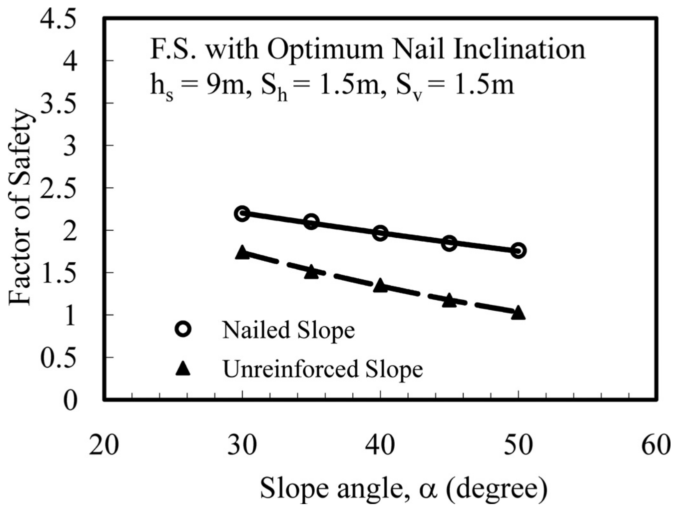

Fig. 13. Influence of slope angle on increase in FS values of soil-nailed slopes

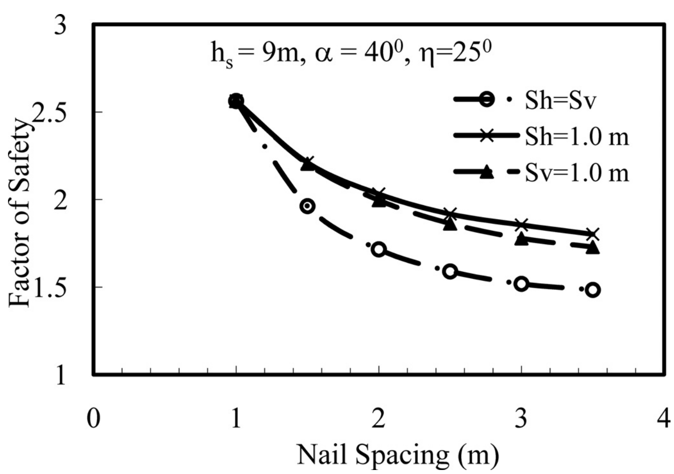

Fig. 14. Effect of nail spacing on FS values of soil-nailed slopes

1-m spacing shall be provided considering drilling for two adjacent nails (Lazarte et al. 2003). Also, for spacing above 2.5 m, some local failures between nails may occur. However, to get more information on the effect of spacing of nails, this study varied the spacing from 1 to 3.5 m. Considering practicality in installation of nails, the top and bottom rows were fixed at 1 m from the slope crest and the bottom of the slope. The nail spacing in between these two rows was varied. In the first case, the spacing was varied equally in both directions (S_h and S_v). In the second case, the horizontal spacing (S_h) of the nails was fixed as 1.0 m, and the vertical spacing (S_v) was varied. In the third case, the vertical spacing (S_v) of the nails was fixed as 1.0 m, and the horizontal spacing (S_h) was varied. The variations of the FS with nail spacing for the three cases are shown in Fig. 14. It can be seen that in all the cases, there was a steep decrease in the FS values with an increase in the nail spacing from 1 to 2.5 m. Beyond a 2.5-m spacing of nails, there were no significant changes in the FS values. It was also observed that the FS values were almost identical in cases where only the horizontal or vertical spacing of the nails was varied up to 2 m; however, beyond 2-m spacing, the reduction in FS resulting from an increase in the vertical spacing was more than that resulting from an increase in the horizontal spacing.

Conclusions

Using the new procedure described in this paper, it is possible to first determine the critical slip surface corresponding to the minimum FS of soil slopes considering 3D failure surfaces. If the slope under consideration is found to have an inadequate FS value, nails can be introduced in the stability analysis for calculation of an enhanced FS value for a nailed slope with the critical slip surface that has been found earlier. The comparison of the FS values for some benchmark problems as obtained from the developed procedure and those reported in the literature and obtained through software programs showed that the developed procedure/computer code gives satisfactory results. For comparison, one LEM-based commercially available program and one SRT-based program were used in this study. In all cases, the FS values obtained from the proposed 3D analysis were found to be higher compared with those obtained by 2D analysis. Very good agreement was found with respect to the location and shape of the slip surfaces as obtained from the present approach and the results obtained from the software and those reported in the literature. Using the developed method, the effect of soil nails oriented at arbitrary angles for a given slope was studied. A computer program was developed for analyzing the problem, which was checked for its correctness. It was found that optimum nail inclination did not remain constant with the angle of the slope but changed with a change in slope angle. For a given slope geometry, soil parameters, and nail inclination, the effect of nail spacing on the FS was also studied. For the given slope, the FS values were found to decrease quickly with an increase in nail spacing from 0.5 to 2.5 m. Beyond 2.5-m spacing of nails, there were no significant changes in FS values.

References

Ahmed, A., Ugai, K., and Yang, Q. Q. (2012). "Assessment of 3D slope stability analysis methods based on 3D simplified Janbu and Hovland methods." *Int. J. Geomech.*, 10.1061/(ASCE)GM.1943-5622.0000117, 81–89.

Anagnosti, P. (1969). "Three-dimensional stability of fill dams." *Proc., 7th Int. Conf. on Soil Mechanics and Foundation Engineering*, International Society for Soil Mechanics and Geotechnical Engineering, London, 275–280.

AutoCAD [Computer software]. Autodesk, San Rafael, CA.

Baligh, M. M., and Azzouz, A. S. (1975). "End effects on stability of cohesive slopes." *J. Geotech. Engrg. Div.*, 101(11), 1105–1117.

Chang, C. S. (1992). "Discrete element method for slope stability analysis." *J. Geotech. Engrg.*, 10.1061/(ASCE)0733-9410(1992)118:12(1889), 1889–1905.

Chen, R. H., and Chameau, J. L. (1983). "Three-dimensional limit equilibrium analysis of slopes." *Géotechnique*, 33(1), 31–40.

Chu, L.-M., and Yin, J. H. (2005). "Comparison of interface shear strength of soil nails measured by both direct shear box tests and pullout tests." *J. Geotech. Geoenviron. Eng.*, 10.1061/(ASCE)1090-0241(2005)131:9(1097), 1097–1107.

Chu, L.-M., and Yin, J. H. (2006). "Study on soil–cement grout interface shear strength of soil nailing by direct shear box testing method." *Geomech. Geoeng.*, 1(4), 259–273.

FLAC/Slope 5 [Computer software]. Itasca Consulting Group, Minneapolis.

GEO5 [Computer software]. Fine Software, Prague, Czech Republic.

Halabian, A. M., Sheikhbahaei, A. M., and Hashemolhosseini, S. H. (2012). "Three-dimensional finite difference analysis of soil-nailed walls under static conditions." *Geomech. Geoeng.*, 7(3), 183–196.

Hossain, M. A., and Yin, J.-H. (2014). "Behavior of a pressure-grouted soil-cement interface in direct shear tests." *Int. J. Geomech.*, 10.1061/(ASCE)GM.1943-5622.0000301, 101–109.

Hovland, H. J. (1977). "Three-dimensional slope stability analysis method." *J. Geotech. Engrg. Div.*, 103(9), 971–986.

Hungr, O. (1987). "An extension of Bishop's simplified method of slope stability analysis to three dimensions." *Géotechnique*, 37(1), 113–117.

Juran, I., Baudrand, G., Farrag, K., and Elias, V. (1990). "Kinematical limit analysis for design of soil-nailed structures." *J. Geotech. Engrg.*, 10.1061/(ASCE)0733-9410(1990)116:1(54), 54–71.

Lagarias, J. C., Reeds, J. A., Wright, M. H., and Wright, P. E. (1999). "Convergence properties of Nelder-Mead simplex method in low dimensions." *SIAM J. Optim.*, 9(1), 112–147.

Lakshminarayana, M. R. (1997). "Three-dimensional stability analysis of nailed soil slopes." Master's thesis, Indian Institute of Technology Kanpur, Kanpur, India.

Lam, L., and Fredlund, D. G. (1993). "A general limit equilibrium model for three-dimensional slope stability analysis." *Can. Geotech. J.*, 30(6), 905–919.

Lazarte, C. A., Elias, V., Espinoza, R. D., and Sabatini, P. J. (2003). "Geotechnical engineering circular no. 7: Soil nail walls." *Rep. No. FHWA0-IF-03-17*, Federal Highway Administration, Washington, DC.

Leshchinsky, D., and Huang, C.-C. (1992). "Generalized three-dimensional slope stability analysis." *J. Geotech. Engrg.*, 10.1061/(ASCE)0733-9410(1992)118:11(1748), 1748–1764.

Maleki, M. R., and Mohammad, M. (2012). "Effect of nail characteristics on slope stability based on limit equilibrium and numerical methods." *Geomech. Geoeng.*, 7(3), 197–207.

MathWorks. (2017). *Optimization toolbox user's guide*, Natick, MA.

MATLAB [Computer software]. MathWorks, Natick, MA.

Patra, C. R., and Basudhar, P. K. (2005). "Optimum design of nailed soil slopes." *Geotech. Geol. Eng.*, 23(3), 273–296.

Pradhan, B., Tham, L. G., Yue, Z. Q., Junaideen, S. M., and Lee, C. F. (2006). "Soil-nail pullout interaction in loose fill materials." *Int. J. Geomech.*, 10.1061/(ASCE)1532-3641(2006)6:4(238), 238–247.

Rotte, V., Viswanadham, B., and Chourasia, D. (2011). "Influence of slope geometry and nail parameters on the stability of soil-nailed slopes." *Int. J. Geotech. Eng.*, 5(3), 267–281.

Sabhahit, N., Basudhar, P. K., and Madhav, M. R. (1995). "A generalized procedure for the optimum design of nailed soil slopes." *Int. J. Numer. Anal. Methods Geomech.*, 19(6), 437–452.

Wei, W. B., and Cheng, Y. M. (2010). "Soil nailed slope by strength reduction and limit equilibrium methods." *Comput. Geotech.*, 37(5), 602–618.

Wei, W. B., Cheng, Y. M., and Li, L. (2009). "Three-dimensional slope failure analysis by the strength reduction and limit equilibrium methods." *Comput. Geotech.*, 36(1–2), 70–80.

Wright, S. G., and Duncan, J. M. (1991). "Limit equilibrium stability analysis for reinforced slopes." *TRB Paper No. 1330*, Transportation Research Board, Washington, DC.

Yuan, J.-X., Yang, Y., Tham, L. G., Lee, P. K. K., and Tsui, Y. (2003). "New approach to limit equilibrium and reliability analysis of soil nailed walls." *Int. J. Geomech.*, 10.1061/(ASCE)1532-3641(2003)3:2(145), 145–151.

Zhang, M., Song, E., and Chen, Z. (1999). "Ground movement analysis of soil nailing construction by three-dimensional (3-D) finite element modeling (FEM)." *Comput. Geotech.*, 25(4), 191–204.